# Visual measurement of the microscopic temperature of porous graphene based on cholesteric liquid crystal microcapsules

Haoyan Jiang (姜浩研)[1], Yaoyi Tang (唐姚懿)[1], Xiaohan Zeng (曾筱涵)[1],
Ruiwen Xiao (肖芮文)[1], Peng Lü (吕 鹏)[1], Lei Wang (王 磊)[1,2,*], and Yanqing Lu (陆延青)[2]

[1]College of Electronic and Optical Engineering & College of Microelectronics, Nanjing University of Posts and Telecommunications, Nanjing 210023, China
[2]National Laboratory of Solid State Microstructures, Key Laboratory of Intelligent Optical Sensing and Manipulation, and College of Engineering and Applied Sciences, Nanjing University, Nanjing 210093, China
*Corresponding author: wangl@njupt.edu.cn

Measuring the microscopic temperature of graphene is challenging. We used cholesteric liquid crystal microcapsules (CLCMs) as temperature sensors to detect the local temperature of three-dimensional porous graphene through quantitative visualization. Based on a CLCM ($\sim$20 μm in size), we determined the temperature variation in a small area with an accuracy of 0.1°C. By analyzing the color changes between two CLCMs, we demonstrated the temperature changes dynamically in a region with a diameter of approximately 110 μm. Furthermore, by comparing the color evolution among the three CLCMs, we visualized the anisotropic thermal properties in the micro-zone. This convenient and low-cost temperature measurement method is expected to further improve graphene-based devices.

Keywords: porous graphene; cholesteric liquid crystal microcapsule; microscopic temperature; visual measurement.

doi: 10.3788/COL202018.031201.

Since graphene was first exfoliated from graphite[1], it has been extensively used in diverse applications, including energy storage[2], single-molecule gas sensors[3], and photovoltaic (PV) cells[4] owing to its unique and superior electrical, thermal, mechanical, optical, and magnetic properties[5–8]. Three-dimensional (3D) porous graphene is a new type of carbon nano-material composed of two-dimensional (2D) graphene on a macroscopic scale. It not only inherits the excellent properties of graphene (including high electrical conductivity, high thermal conductivity, and chemical stability), but it also has high specific surface area, high porosity, excellent compressibility, and an interconnected conductive network owing to its special 3D micro-nano structure. This makes it attractive for applications such as flexible electronic equipment[9], thermal engineering[10], and catalysis loading[11]. With the miniaturization and integration of devices, it is important to investigate the microscopic thermal properties to improve their performance. 3D porous graphene can serve as an excellent material for heat transfer in energy storage and optoelectronic devices. However, accurately measuring the microscopic temperature of graphene is challenging.

Conventional temperature measurement methods, such as thermocouples, thermistors, optical fiber based temperature sensors, and infrared thermometers[12–14], cannot accurately distinguish the microscopic temperature distribution with a high spatial resolution and high temperature sensitivity. Different approaches have been proposed to develop ultra-small thermal sensors for microscopic temperature measurement. These approaches include temperature sensors based on carbon nanotubes (CNTs)[15]; however, the resistance thermometer may not work if the chosen CNTs are semi- or non-conductive ones. ElShimy et al. fabricated a nano sensor through focused ion beam chemical vapor deposition (FIB-CVD) of tungsten over atomic force microscope (AFM) cantilevers to detect heat[16]. Zhong et al. measured the magnetization of magnetic nanoparticles and obtained local temperature information through a certain model[17]. Oh et al. developed an optical approach to measure the temperature distribution by exploiting the temperature dependency of the water refractive index (RI)[18]. However, it cannot be used for the microscopic temperature measurement of graphene. An in-situ near-infrared (NIR) charge coupled device (CCD) imaging system has been developed for measuring the temperature distribution of graphene during heating[19]. Although these methods provide a high spatial resolution, they are expensive, complicated, and not intuitive enough, making them unsuitable for practical applications, particularly for 3D porous graphene.

A cholesteric liquid crystal (CLC) is a type of liquid crystal that is sensitive to temperature. As such, the selective reflection wavelength of a CLC varies with its helix pitch due to small temperature variations. The color change can be directly observed in the visible band, making the CLC an ideal temperature sensor[20]. Although it is not stable, the encapsulation technique, which is a promising protective method, can be applied to overcome

this issue[21]. A cholesteric liquid crystal microcapsule (CLCM) has been used in various optical applications without requiring electricity or orientation alignment including in flexible displays, secure authentication, and 3D omnidirectional microlasers[22]. However, this technique has not been applied to the thermal sensing of graphene.

Herein, we propose a straightforward approach to measure the microscopic temperature of 3D porous graphene through a cheap and simple fabrication process. We first combine the 3D porous graphene with CLCMs, which are ultra-small, temperature-supersensitive thermal sensors. A microscopy imaging system is utilized to analyze the color change of the CLCMs and thus determine the temperature of the graphene with a spatial resolution of approximately 20 μm and a temperature sensitivity of 0.1°C. Finally, the dynamic change in the temperature and anisotropy at the microscopic level are demonstrated quantitatively.

Figure 1 shows the setup of the visual measurement system used for measuring the microscopic temperature of porous graphene. It mainly consists of a CMOS camera (JC-HD200S), an imaging lens (JC-TZ01), an auxiliary objective lens (JC-FZ10X), a temperature controller, a display, a computer, and a mouse. The CMOS camera paired with the microscopic lens helps take high-resolution images of extremely small component features, with magnifications ranging from 10× to 100×. The temperature controller is a type of semiconductor refrigeration component (PA-075-24, Pengnan Technology Co., Ltd.), which provides high-precision temperature control (accuracy: 0.1°C). We used the mouse to select a position on the sample and showed its temperature on the display. The computer was used for image processing. The 3D porous graphene including the CLCMs is placed on the temperature controller, as shown in the inset of Fig. 1. The thickness of the 3D porous graphene is ∼0.5 mm.

The temperature can be detected through the notable changes in the color of the CLCMs by the naked eye. When the wavelength of the incident light ($\lambda_0$) matches the pitch ($p$) of the CLCMs, i.e., $\lambda_0 = n \times p$ ($n$ is the average refractive index of the CLCMs), the light at this wavelength will be reflected. The temperature can be judged from the color of the reflected light. The CLCMs

distributed within the porous graphene are illuminated from above with white LED, and the reflection is monitored using the microscopic imaging system. The measurement system exhibits a high-resolution sensing capability in space as well as in temperature, as the diameter of the CLCMs is on the order of only 10 μm with a temperature precision of 0.1°C. Even a relatively small change in the temperature can lead to strong variations in the color in the visible light. In addition to quickly and easily determining the temperature of the microscopic areas of graphene, this method can be used to visualize the heat transfer through the 3D porous graphene by analyzing the different CLCMs.

The quality of the 3D graphene film was characterized by a Raman spectrum, as shown in Fig. 2(a). The G peak position is 1580 cm$^{-1}$, representing the symmetry-allowed graphite band; D (1350 cm$^{-1}$) is disorder-induced, and 2D (2700 cm$^{-1}$) is the second harmonic band of D. The G-to-2D peak intensity ratio is consistent with that observed for 3D porous graphene[23]. The CLCMs (RM2325, Japan Capsular Products) and methyl silicone oil are mixed at a mass ratio of 1:1.5 and then uniformly stirred using a magnetic stirrer. A small amount of the mixture is poured onto the surface of the 3D porous graphene. According to the imaging system, the diameter of the pores of the graphene is ∼100 μm and the CLCMs have an average diameter of 20 μm.

Figures 2(b)–2(d) show the color change of the CLCMs at different temperatures. Here, we study three images. As the temperature increases, the CLCMs gradually turn blue from red at 22, 23.2, and 24.9°C, respectively. Different temperatures can be detected based on the color as heat is conducted from the graphene. Thus, the temperature in the ∼20 μm area can be determined. The CLCMs exhibit slightly different colors because of the nonuniform particle size, different observation angles, and different locations at which they are placed[22]. The 3D porous graphene itself exhibits a black color as it absorbs all the
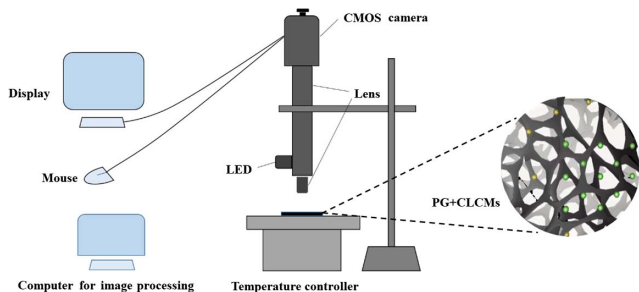


Fig. 1. Visual system for microscopic temperature measurement of porous graphene based on CLCMs. The inset shows the distribution of CLCMs on the porous graphene.
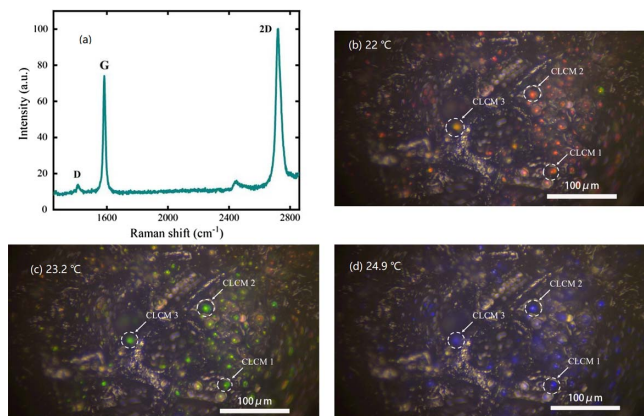


Fig. 2. Characteristics of graphene and CLCMs: (a) Raman spectrum of 3D graphene; (b)–(d) microscopic images of 3D porous graphene with CLCMs at 22, 23.2, and 24.9°C, respectively.

visible light, making it beneficial in detecting the light that is reflected from the CLCMs.

To visually measure the microscopic temperature of the 3D porous graphene based on the CLCMs, first, the hue of the image-based temperature calibration is required. The hue increases monotonically when the color changes. This is convenient to quantify the color change of the CLCMs[24–26]. We selected three CLCMs to map the temperature to the hue value that are used later to detect the thermal properties of the porous graphene. The eyedropper tool of Photoshop was used to extract the RGB value of a CLCM color image. The RGB was then converted to hue. The hue values at different temperatures were fitted to the curves using MATLAB. We measured the color change of the CLCMs using a hot stage, the temperature of which was controlled from 21.5 to 25°C in intervals of 0.1°C. We waited for 20 s each time when the temperature changed to ensure thermal equilibrium. To avoid any inconsistency in the measurement, the hue value was obtained by averaging the results of multiple measurements. Figure 3 shows the temperature calibration curves for the three different CLCMs. The curves are similar but not exactly the same, because of the reasons given previously. Based on the relationship between the hue value of the CLCMs and the temperature value, we can determine the temperature at a specific position on the porous graphene. As the hue is calibrated at 0.1°C intervals, the microscopic temperature of graphene can be obtained accurately with an accuracy of 0.1°C.

To demonstrate the microscopic thermal properties of porous graphene, we used an LED to heat the lower right side of the porous graphene, which is not shown in Fig. 4. As graphene has an excellent thermal conductivity, the heat rapidly transmits through the porous graphene to the cold side, passing through CLCM 1 first, then CLCM 2 and CLCM 3, and finally reaches thermal equilibrium while the colors of the CLCMs attached to the graphene surface change with temperature. Figures 4(a)–4(d) show that the CLCMs turn green from red with a gradual increase in the temperature.

Combined with the temperature–time curve shown in Fig. 4(e), we analyze the color of a single CLCM to determine the related microscopic temperature of the 3D porous graphene based on the calibration (Fig. 3). For example, the temperature of graphene with CLCM 1 changes faster than that with CLCM 2 and CLCM 3, from
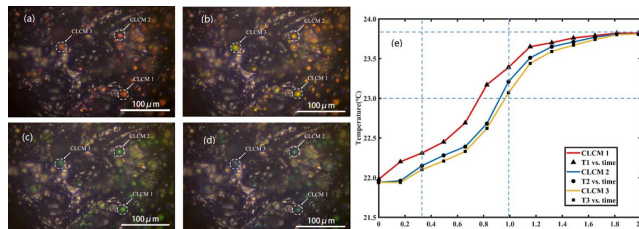


Fig. 4. Visual measurement of the microscopic temperature of porous graphene based on CLCMs when the heat transfers from the lower right corner of the porous graphene: images of CLCMs embedded in the porous graphene at the initial temperature when (a) $T = 0$ s; (b) $T = 0.33$ s; (c) $T = 1$ s; (d) $T = 2$ s from the video taken by the microscopy imaging system; (e) temperature dependence on the time for the three CLCMs ($T$: time).

about 22 to 23.8°C. CLCM 1 reaches 23°C faster than CLCM 2 and CLCM 3, as indicated by the dashed line in Fig. 4(e).

The dynamic thermal transfer behavior of the porous graphene at the microscopic level can be addressed by analyzing the color changes between two CLCMs. The distance between CLCM 1 and CLCM 2 is approximately 110 μm. Figure 4(e) shows that the temperature of CLCM 1 is higher than that of CLCM 2 when $T = 0.33$ s [the image shown in Fig. 4(b)]. Even when $T = 1$ s, CLCM 1 is at a higher temperature. Figure 4(c) shows that the CLCMs turn green. Thus, we demonstrate the temperature changes dynamically in a region having a diameter of approximately 110 μm.

Finally, to characterize the heat transfer ability in different directions, we evaluated the system with three CLCMs. The curves in Fig. 4(e) show that the heat transfer is faster from CLCM 1 to CLCM 2 than to CLCM 3. Therefore, we concluded that the thermal conductivity is anisotropic at the microscopic level. The primary cause could be the anisotropy of graphene. After 2 s, they reach thermal equilibrium, as shown in Fig. 4(d). This implies that the temperature of the whole area is ~23.8°C. Owing to the excellent thermal conductivity of the 3D porous graphene, the transient temperature evolution process can be studied more elaborately using a camera with a higher frame rate.

3D porous graphene, as a lightweight, freestanding, high thermal conductivity, and large specific surface area material, has good potential in the development of various graphene-based devices. To make full use of this material, we studied its microscopic temperature properties. We leverage a temperature-supersensitive CLCM (~20 μm), the color change of which could be detected to visually measure the microscopic temperature of porous graphene with an accuracy of 0.1°C. Moreover, CLCMs change their color owing to their wide angle, broad bandwidth, and highly efficient visible light absorption characteristics. The dynamic change in the temperature in an area of diameter 110 μm and the anisotropic heat conductivity of the porous graphene were determined by analyzing
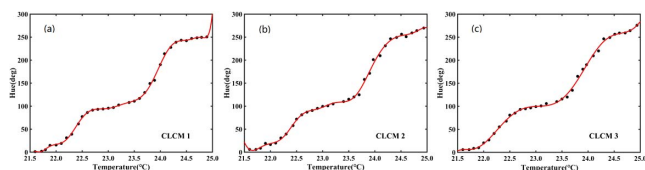


Fig. 3. Temperature dependence on the hue of (a) CLCM 1, (b) CLCM 2, and (c) CLCM 3. The points indicate the experimental data, and the solid lines indicate the fitting curves of the temperature calibration for hue.

the color change of one, two, and three CLCMs, with a spatial resolution of 20 μm and a temperature sensitivity of 0.1°C. Our findings may have promising applications in the thermal management of graphene devices. The proposed solution also paves a way for the microscopic temperature measurement of other 2D and 3D materials. Future studies can be focused on determining the thermal performance at arbitrary positions with a high precision and wide temperature range.

## References

1. K. S. Novoselov, A. K. Geim, S. V. Morozov, D. Jiang, Y. Zhang, S. V. Dubonos, I. V. Grigorieva, and A. A. Firsov, Science **306**, 666 (2004).
2. Y. Zhu, S. Murali, M. D. Stoller, K. J. Ganesh, W. Cai, P. J. Ferreira, A. Pirkle, R. M. Wallace, K. A. Cychosz, M. Thommes, and D. Su, Science **332**, 1537 (2011).
3. S. Garaj, W. Hubbard, A. Reina, J. Kong, D. Branton, and J. A. Golovchenko, Nature **467**, 190 (2010).
4. L. Gomez De Arco, Y. Zhang, C. W. Schlenker, K. Ryu, M. E. Thompson, and C. Zhou, ACS Nano **4**, 2865 (2010).
5. A. K. Geim and K. S. Novoselov, Nat. Mater. **6**, 183 (2007).
6. A. K. Geim, Science **324**, 1530 (2009).
7. A. A. Balandin, S. Ghosh, W. Bao, I. Calizo, D. Teweldebrhan, F. Miao, and C. N. Lau, Nano Lett. **8**, 902 (2008).
8. T. Low and P. Avouris, ACS Nano **8**, 1086 (2014).
9. L. Jiang and Z. Fan, Nanoscale **6**, 1922 (2014).
10. H. Ghasemi, A. Rajabpour, and A. H. Akbarzadeh, Int. J. Heat Mass Transfer **123**, 261 (2018).
11. H. R. Byon, J. Suntivich, and Y. Shao-Horn, Chem. Mater. **23**, 3421 (2011).
12. S. Sade, L. Nagli, and A. Katzir, Appl. Phys. Lett. **87**, 101109 (2005).
13. X. Wang, Y. Guo, and L. Xiong, Chin. Opt. Lett. **16**, 070604 (2018).
14. H. Li, Q. Zhao, S. Jiang, J. Ni, and C. Wang, Chin. Opt. Lett. **17**, 040603 (2019).
15. V. T. S. Wong and W. J. Li, in *Proceedings of the Sixteenth Annual Conference on Micro Electro Mechanical Systems* (2003), p. 41.
16. H. M. ElShimy, M. Nakajima, F. Arai, and T. Fukuda, in *IEEE Conference on Nanotechnology* (2007), p. 1045.
17. J. Zhong, W. Liu, Z. Du, P. César de Morais, Q. Xiang, and Q. Xie, Nanotechnology **23**, 075703 (2012).
18. J. T. Oh, G. H. Lee, J. Rho, S. Shin, B. J. Lee, Y. Nam, and Y. K. Park, Phys. Rev. Appl. **11**, 044079 (2019).
19. T. Saito, R. Suda, and J. Shirakashi, in *IEEE International Conference on Nanotechnology* (2013), p. 717.
20. T. E. Cooper, R. J. Field, and J. F. Meyer, J. Heat Transfer **97**, 442 (1975).
21. S. S. Lee and S. H. Kim, Macromol. Res. **26**, 1054 (2018).
22. M. Schwartz, G. Lenzini, Y. Geng, P. B. Rønne, P. Y. A. Ryan, and J. P. F. Lagerwall, Adv. Mater. **30**, 1707382 (2018).
23. H. Bi, I. W. Chen, T. Lin, and F. Huang, Adv. Mater. **27**, 5943 (2015).
24. Y. Tadokoro, T. Nishikawa, B. Kang, K. Takano, M. Hangyo, and M. Nakajima, Opt. Lett. **40**, 4456 (2015).
25. J. Stasiek, A. Stasiek, M. Jewartowski, and M. W. Collins, Opt. Laser Technol. **38**, 243 (2006).
26. J. W. Baughn, M. R. Anderson, J. E. Mayhew, and J. D. Wolf, J. Heat Transfer **121**, 1067 (1999).